Joint Power/Rate Control and Channel Assignment in Cognitive Radio Networks: A Multi-level Spectrum Opportunity Perspective

Tao Shu and Marwan Krunz
Department of Electrical and Computer Engineering
University of Arizona

September 1, 2008

Abstract

In a cognitive radio network (CRN), the spectrum opportunities should be efficiently utilized through careful coordination between cognitive radio (CR) users. In this paper, we formulate the coordinated channel access as a joint power/rate control and channel assignment optimization problem, with the objective of maximizing the sum-rate achieved by all CRs over all channels. The problem is formulated under a generalized multi-level spectrum opportunity framework, which reflects the *microscopic* spatial opportunity available for CRs. Both centralized and distributed approximate algorithms to the problem are developed. We prove that the distributed algorithm can achieve a certain fraction of the optimal throughput, while the centralized algorithm gives a tight upper bound on the optimal solution. We apply our algorithms to a spectrum-leasing application, and demonstrate the throughput gain of the multi-level spectrum opportunity structure over the conventional binary structure while taking the overhead into account. Numerical results verify the accuracy of our algorithms and the significant gain achieved by the multi-level framework.

1 Introduction

Cognitive radio networks (CRNs) have recently received a substantial amount of interest as a means of improving spectrum utilization. Aiming at opening up the under-utilized sectors of the licensed spectrum for secondary reuse, cognitive radios (CRs) can dynamically access a channel, provided that their communications do not cause harmful interference to the licensed users of that channel (a.k.a., the primary radios (PRs)). The operation of a CRN needs to address two essential problems: (1) discovery of spectrum opportunities, i.e., idle channels that can be used by CRs, and (2) efficient reuse of such opportunities. While numerous studies have been dedicated to the first problem based on channel sensing techniques, the second problem remains a challenge in a multi-CR environment. This is because different CRs may sense the same channel and determine it to be available. Therefore, channel access needs to be carefully coordinated between these CRs to avoid collisions and more importantly, ensure efficient utilization of the spectrum opportunity from a network-wide point of view.

In this work, we study the coordinated channel access problem between CRs by formulating it as a joint power/rate control and channel assignment optimization problem. Given the available channels at different CRs, we need to specify for each CR which channels it should transmit on and what powers and rates it should use on these channels. We are interested in both centralized (for better performance) and distributed (for better implementablility) solutions. In contrast to previous work that aims at maximizing the information-theoretic capacity of the system, in this work our objective is to maximize the sum-rate achieved by each CR. Unlike the information-theoretic capacity that is defined as a logarithmic function of the received signal-to-interference-plus-noise ratio (SINR), the rate in our setup depends on the PHY-layer implementation. In other words, our problem has a wider scope and can be applied to any arbitrarily given rate-SINR function.

Coexistence between PRs and CRs in the same system also gives rise to a new structure for our problem. Two new types of interference need to be accounted for: PR-to-CR interference and CR-to-PR interference. The latter is more critical and should be constrained, because it directly influences PRs' operation. For each CR and each channel, we adopt a *power mask* to describe the maximum transmission power the CR can use without causing unacceptable interference to neighboring PRs. By nature, this power mask is *multi-level*. For example, consider the scenario in Figure 1, where two PR links ($a \rightarrow b$ and $c \rightarrow d$) and one CR link (CR1 $\rightarrow$ CR2) exist in the same vicinity and share the same frequency channel. CR1 can transmit as far as its received power at the closest active PR receiver is smaller than the PR's interference tolerance, for which we assume a small value for all the PRs. So depending on the status (ON/OFF) of the PR links, CR1's power mask takes one of three levels: $\frac{\text{PR's interference tolerance}}{h_{1b}}$ (Level 1), $\frac{\text{PR's interference tolerance}}{h_{1d}}$ (Level 2), and $P_{\max}$ (Level 3, the full power supported by the CR's battery), where h_{ij} is the channel gain between nodes i and j, and the circles denote the interference ranges of various levels. Note that this multi-

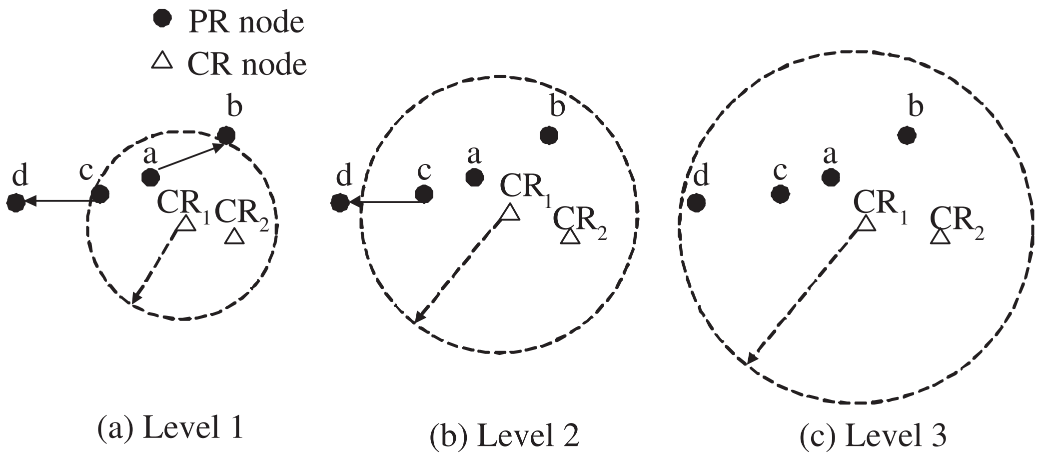

Figure 1: An example of the multi-level spectrum opportunity.

level structure is a generalization of the widely-used *binary* structure, whereby the power mask is 0 if any of the PR neighbors is active, or $P_{\max}$ if none of its PR neighbors is active. We realize that this multi-level structure reflects the *microscopic* spatial opportunity for CRs, and can be potentially exploited to increase the CRN's throughput. So we attempt to accommodate this general form of spectrum opportunity in our optimization. Consequently, our formulation becomes more complicated, because now the same channel may present different levels of availability to different CRs.

The multi-level structure of the power mask makes the widely-used SINR-based approximation unapplicable to our problem. For example, in many existing power/rate control and channel assignment problems, a convex formulation is obtained through the capacity approximation $\log(1 + \text{SINR}) \approx \text{SINR}$ if $\text{SINR} \ll 1$ (low-SINR regime, e.g., see [12]) or $\log(1 + \text{SINR}) \approx \log(\text{SINR})$ if $\text{SINR} \gg 1$ (high-SINR regime, e.g., see [16]). However, now a CR is expected to operate over a wide range (low-, mid-, and high-) of SINR regimes over time due to the multiple levels of the power mask. Even at a time instance, different CRs may be operating in different SINR regimes. Therefore, those approximation techniques adopted separately for low- and high-SINR regimes are no longer appropriate here. A new SINR-independent treatment is needed for the problem.

The contributions of this work include the following. We first show that the joint power/rate control and channel assignment problem can be formulated as a mixed integer nonlinear programming (MINLP) problem that is NP-hard. By exploiting the discrete set of rates supported by the CR on each channel, we transform this MINLP to a binary linear programming (BLP) problem that only contains binary variables and linear objective function and constraints. This transformation applies to any arbitrarily given rate-SINR relationship, but at a cost of increased number of variables. We then develop two polynomial-time approximate algorithms for the BLP. The first one is the centralized *LPSF* algorithm. It is based on iteratively solving a series of linear programming problems and sequentially fixing the variables to either 1 or 0 in each iteration. The second is the distributed *EF-based* algorithm. It involves iterative and on-line adjustment of the power/rate of each CR over each channel based on some *economic factor* that accounts for the efficiency of investing power on a given channel. We show that this distributed algorithm is provably efficient, i.e., it can achieve a provable fraction of the optimal performance. As a byproduct, the centralized algorithm gives an upper bound on the optimal solution. This further allows us to explicitly evaluate the performance gap between the approximate solutions and the optimal one in each realization. Simulation results are used to verify the accuracy of the LPSF and EF algorithms, showing that the actual performance gap is less than 10% in all simulated realizations.

To evaluate the benefit brought by the multi-level spectrum opportunity, we subsequently apply our algorithms to a spectrum-leasing system, whereby a CRN shares the spectrum with an infrastructured PR network (PRN). We illustrate how the multi-level spectrum opportunity can be calculated under the assistance of a broadcast-subscription mechanism. The interesting question is how much gain the multi-level spectrum opportunity scheme can attain over the conventional binary scheme, with the overhead of the calculation being accounted for. We evaluate this gain against various parameters associated with the overhead. Our numerical results show that significant gain (e.g., over 100% at best) can be achieved by the multi-level scheme after discounting the overhead.

The rest of this paper is organized as follows. We review the related work in Section 2. We describe the models and formulate the optimization problem in Section 3. The transformation to BLP formulation, the LPSF, and the EF algorithms are presented in Section 4. We apply our algorithms to the infrastructured PRN/CRN system in Section 5. Simulation evaluation and discussion are provided in Section 6 and we conclude the work in Section 7.

2 Related Work

Much of the related work is based on the binary-type spectrum opportunity. Early works provide collision-free channel assignment for CR nodes given a set of available channels at each node. This problem can be described as an interference-graph vertex-coloring problem [14, 22]. To obtain a fast solution, various distributed approximations were proposed, which are based on observing local interference patterns [21], local bargaining [1], or on coordinations between CR nodes that aim at maximizing some system utility [2][18]. Because of the graph-theoretic nature of these algorithms, they take transmission power as input rather than output, and thus are not applicable to power/rate control problems.

The second body of work considers the sensing/channel access decision-making process from a single CR's viewpoint. This is also termed as *MAC-layer sensing*. Existing works include the partially observable Markov decision process (POMDP) model [20], the constrained Markov decision processes (CMDPs) model [19], and the optimal stopping-rule models [3] [7]. Assuming a semi-Markov process for the PR traffic, Kim and Shin [8] proposed a sensing-period adaptation algorithm that maximizes the discovery of spectrum opportunities and minimizes the delay in finding an available channel. Based on a similar PR traffic model, the authors in [6] studied a dynamic access scheme subject to a constraint on the CR-to-PR violation rate, but only for a system of one PRN and one CR link. The coordinated use of spectrum opportunities at neighboring CRs has not been considered in these works, and collisions between CR transmissions are resolved using standard CSMA/CA techniques. Such treatment leads to non-optimal performance from a network's viewpoint.

The third type of work simplifies the problem by restricting the treatment to CR nodes only. So the CR-to-PR and PR-to-CR interferences do not appear in their formulation. Within this category, Hou et al. [5] considered the joint optimization of spectrum, scheduling, and routing in a multi-hop software-defined-radio (SDR) network. Yi and Hou studied the joint optimization of power control, scheduling, and routing for a multi-hop SDR network in [10] (for a centralized algorithm) and [11] (for a distributed algorithm). Yuan et al. [17] introduced the concept of time-spectrum blocks to study spectrum allocation in CRNs. Based on a continuous-time Markov model, Xing et al. [15] proposed a random access protocol that achieves airtime fairness among CRs. The work in [16] considers spectrum access for CRs under an interference temperature constraint. However, because this constraint is defined only at a single location, compliance to it does not necessarily prevent interference on PR nodes.

3 System Model and Problem Formulation

We consider a distributed (ad hoc) CRN that coexists with M legacy (fixed spectrum) PRNs over a finite area. PRN m, $m = 1, \ldots, M$, is licensed to operate over its own frequency channel of bandwidth B_m. In reality, a PRN may occupy more than one frequency channel. Such a network can be easily captured in our model by using multiple (virtual) PRNs that operate over different channels.

Let the number of CR links in the system be N. A CR link refers to a pair of CR sender and a CR receiver. For CR link i, we denote the sender and the receiver by $S(i)$ and $D(i)$, respectively. A CR link can transmit over multiple non-contiguous channels simultaneously. Let the transmission power on channel m be $P_i^{(m)}$. To avoid unacceptable CR-to-PR interference, this transmission power must be constrained below certain power mask $\hat{P}_i^{(m)}$. The value of $\hat{P}_i^{(m)}$ is related to the status of neighboring PRs and thus changes over time. For now, we assume that the value of $\hat{P}_i^{(m)}$s, $i = 1, \ldots, N$ and $m = 1, \ldots, M$, are given in each snapshot as input parameters of the joint power/rate control and channel assignment problem. We consider the calculation of $\hat{P}_i^{(m)}$ in Section 5.

We stick to the *protocol model* for the collisions between CRs. We say that CR links i and j are interfering links on channel m if $\hat{P}_i^{(m)} h_{S(i)D(j)} > P_{I,CR}$ or $\hat{P}_j^{(m)} h_{S(j)D(i)} > P_{I,CR}$, where $h_{S(i)D(j)}$ and $h_{S(j)D(i)}$ are the cross-link channel gains of the two links, and $P_{I,CR}$ is a small fixed value, denoting the sensitivity of the CR receiver. Any received power below $P_{I,CR}$ can be deemed as ignorable in terms of interference. We assume that an exclusive channel occupancy policy is used to resolve collision between CRs: For any two interfering CR links on channel m, only one of them can access the channel at any given time.

Treating interference as noise, the rate of CR link i on channel m is given by

$$R_i^{(m)} = B_m f\left(\frac{P_i^{(m)} h_i^{(m)}}{q_{D(i)}^{(m)} + N_0}\right) \tag{1}$$

where f is any arbitrary rate-SINR function decided by the PHY-layer implementation, $h_i^{(m)}$ is the channel gain of link i on channel m, $q_{D(i)}^{(m)}$ is the received interference over channel m at $D(i)$, and N_0 is the AWGN. Because an exclusive channel occupancy policy is used, the interference $q_{D(i)}^{(m)}$ only comes from active co-channel PRs and can be measured by the CR receiver $D(i)$ on line.

For $i = 1, \ldots, N$ and $m = 1, \ldots, M$, define variables

$$x_i^{(m)} \stackrel{\text{def}}{=} \begin{cases} 1, & \text{if channel } m \text{ is used by CR link } i \text{, i.e., } R_i^{(m)} > 0 \\ 0, & \text{otherwise} \end{cases} \tag{2}$$

Our objective is to maximize the sum of rate of all CR links over all channels in current snapshot, i.e.,

$$\text{maximize} \sum_{i=1}^{N} \sum_{m=1}^{M} x_i^{(m)} R_i^{(m)} \tag{3}$$

where the maximization is to be carried out with respect to $x_i^{(m)}$'s and $R_i^{(m)}$'s.

A CR link i should satisfy the following constraints:

C1: CR-to-PR constraint: The transmission power of link i on channel m should not exceed the power mask $\hat{P}_i^{(m)}$. From (1), this constraint can be written in terms of $R_i^{(m)}$ as

$$\frac{1}{h_i^{(m)}}(q_{D(i)}^{(m)} + N_0) f^{-1}(r_i^{(m)}) \leq \hat{P}_i^{(m)}, \quad m = 1, \ldots, M \tag{4}$$

where f^{-1} is the inverse function of f, and $r_i^{(m)} = \frac{R_i^{(m)}}{B_m}$ is the spectrum efficiency of link i on channel m.

C2: Power supply constraint: The sum of the transmission powers over all channels should not exceed the maximum power provided by the battery, i.e.,

$$\sum_{m=1}^{M} \frac{1}{h_i^{(m)}}(q_{D(i)}^{(m)} + N_0) f^{-1}(r_i^{(m)}) \leq P_{\max,i}. \tag{5}$$

C3: CR-to-CR collision constraint: If channel m is being used by CR link i, then it cannot be used by another CR link that interferes with link i on channel m, and vice versa:

$$x_i^{(m)} + x_j^{(m)} \leq 1, \quad \forall j \in I_i^{(m)} \tag{6}$$

where $I_i^{(m)} = \left\{ j : j \neq i, \hat{P}_i^{(m)} h_{S(i)D(j)}^{(m)} > P_{I,CR} \right\} \cup \left\{ j : j \neq i, \hat{P}_j^{(m)} h_{S(j)D(i)}^{(m)} > P_{I,CR} \right\}$ is the set of interfering CR links of link i on channel m.

C1 to C3 are the basic constraints that apply to all CRNs. Additional constraints may exist depending on the CR's PHY-layer implementation. For simplicity, we only include C1 to C3 to our formulation at this point. We will discuss other constraints in Section 4.4.

4 Solutions

4.1 Transformation to BLP

An observation of the objective function (3) and the constraints C1-C3 shows that this formulation constitutes a *mixed integer nonlinear programming (MINLP)* problem. The solution to such a problem is NP-hard, in general. To make this formulation more amenable for further processing, we exploit the fact that actual communication systems only support a finite set of discrete transmission rates on each channel. Denote this set of rates by $\mathbf{U} = \{0, u_1, u_2, \ldots, u_K\}$ (in b/s/Hz), where $0 < u_1 < \ldots < u_K$. Define $\gamma_k \stackrel{\text{def}}{=} f^{-1}(u_k)$ for $k = 1, \ldots, K$; γ_k is the received symbol energy to interference plus noise density ratio (E_S/I_0) required to support the kth rate under the power-rate relationship defined by (1). Let $C_i^{(m)} \stackrel{\text{def}}{=} \frac{1}{h_i^{(m)}}\left(q_{D(i)}^{(m)} + N_0\right)$ for $i = 1, \ldots, N$ and $m = 1, \ldots, M$. $C_i^{(m)}$ is a known quantity for each CR link on each channel. We further define a new variable $y_{k,i}^{(m)}$ for all $k = 1, \ldots, K$, $i = 1, \ldots, N$, and $m = 1, \ldots, M$:

$$y_{k,i}^{(m)} \stackrel{\text{def}}{=} \begin{cases} 1, & \text{if link } i \text{ is transmitting on channel } m \text{ using rate } u_k \\ 0, & \text{otherwise.} \end{cases} \tag{7}$$

In addition, we add the following constraint on $y_{k,i}^{(m)}$:

$$\sum_{k=1}^{K} y_{k,i}^{(m)} \leq 1. \tag{8}$$

which accounts for the fact that a link can use at most one rate on a given channel at a time. It is easy to show that the following relation holds:

$$x_i^{(m)} = \sum_{k=1}^{K} y_{k,i}^{(m)}. \tag{9}$$

Similarly, we can rewrite the spectrum efficiency $r_i^{(m)}$ in terms of $y_{k,i}^{(m)}$ and u_k:

$$r_i^{(m)} = \sum_{k=1}^{K} u_k y_{k,i}^{(m)}. \tag{10}$$

Substituting (9) and (10) into (3) through (6), we get the following equivalent formulation to the original MINLP problem:

$$\begin{array}{lll} & \text{maximize} & \sum_{i=1}^{N}\sum_{m=1}^{M}\sum_{k=1}^{K} B_m u_k y_{k,i}^{(m)} \\ & \text{such that} & \\ \tilde{C}1: & & C_i^{(m)}\sum_{k=1}^{K}\gamma_k y_{k,i}^{(m)} \leq \hat{P}_i^{(m)} \\ \tilde{C}2: & & \sum_{m=1}^{m} C_i^{(m)}\sum_{k=1}^{K}\gamma_k y_{k,i}^{(m)} \leq P_{\max,i} \\ \tilde{C}3: & & \sum_{k=1}^{K} y_{k,i}^{(m)} + \sum_{k=1}^{K} y_{k,j}^{(m)} \leq 1, \quad \forall j \in I_i^{(m)} \end{array} \tag{11}$$

where the maximization is w.r.t. the $y_{k,i}^{(m)}$'s.

An examination of (11) shows that the former MINLP problem has been transformed into a binary linear program (BLP) that contains only binary variables and linear objective function and constraints. A nice property of (11) is that the rate levels u_k, $k = 1, \ldots, K$, and the corresponding γ_k's are fed into the BLP formulation as tuples (u_k, γ_k). In other words, the BLP formulation does not rely on the specific functional relationship between u_k and γ_k, and thus can accommodate any arbitrary rate-power relation (e.g., a staircase-like function that characterizes practical multi-rate systems).

4.2 LPSF Centralized Algorithm

A BLP is a combinatorial problem. Its solution, in general, is NP-hard. A typical algorithm to approximately solve this problem is the so-called *branch-and-bound* algorithm, whose worst-case time complexity is exponential.

Instead of employing a branch-and-bound algorithm, we develop polynomial-time approximate algorithms by exploiting the special structure of the problem. An observation of (11) indicates that if we relax $y_{k,i}^{(m)}$'s from their binary values and allow them to take real values between 0 and 1, then the formulation becomes a linear program (LP) that is solvable in polynomial time. In addition, the constraint $\tilde{C}3$ dictates that if for some m, k, and i, $y_{k,i}^{(m)} = 1$, then $y_{h,i}^{(m)} = 0$ for all $h \neq k$ and $y_{l,j}^{(m)} = 0$ for all $j \in I_i^{(m)}$ and $1 \leq l \leq K$. In other words, a strong dependence exists between the $y_{k,i}^{(m)}$'s that belong to the same interfering CR link set. The main idea behind our fast approximate solution is to fix the values of $y_{k,i}^{(m)}$'s sequentially through solving a series of relaxed LP problems, with at least one $y_{k,i}^{(m)}$ finalized to a binary value at each iteration.

Our approximation algorithm, called LP with sequential fixing (LPSF), is described in Table 1. In the first iteration, we append the constraint $0 \leq y_{k,i}^{(m)} \leq 1$ to (11) and relax all $y_{k,i}^{(m)}$'s to real values between 0 and 1. We refer to the resulting formulation as $\mathrm{LP}^{(1)}$, which must have a feasible solution according to Lemma 1. The solution to $\mathrm{LP}^{(1)}$ is an upper bound on the optimal solution to (11), because the feasibility region of the BLP is a subset of that of $\mathrm{LP}^{(1)}$. However, the solution of $\mathrm{LP}^{(1)}$ is, in general, not a feasible solution to the original BLP problem, because the $y_{k,i}^{(m)}$'s can now take values between 0 and 1. Among all $y_{k,i}^{(m)}$'s, we pick the one that has the largest value, and we denote this $y_{k,i}^{(m)}$ by $Y_{k,i}^{(m)}$ for ease of identification. We set $Y_{k,i}^{(m)} = 1$. Accordingly, all $y_{h,i}^{(m)}$'s for $h \neq k$ and all $y_{l,j}^{(m)}$'s for $j \in I_i^{(m)}$ and $1 \leq l \leq K$ must now be set to 0. Substituting these $y_{k,i}^{(m)}$'s with their fixed values into the LP$^{(1)}$, we get a new LP, called LP$^{(2)}$, whose variables do not include those that have been fixed after the execution of LP$^{(1)}$ (such variables have been replaced by their binary values). A feasibility check is then conducted on LP$^{(2)}$. If the feasible region of LP$^{(2)}$ is empty, that means the first fixing in this iteration, i.e., $Y_{k,i}^{(m)} = 1$, is not correct. So we reset $Y_{k,i}^{(m)}$ to 0. This change means all those variables that belong to the same interfering CR link set as $Y_{k,i}^{(m)}$ and whose values have been fixed to 0 in this iteration must now become variables. The revised fix, i.e. $Y_{k,i}^{(m)} = 0$, is then substituted into LP$^{(1)}$, giving rise to LP$^{(3)}$. LP$^{(3)}$ must be feasible (see Lemma 2). In a nutshell, at this point we either have a feasible LP$^{(2)}$ or have a feasible LP$^{(3)}$. In either case, the new feasible formulation is renamed as LP$^{(1)}$ and a new iteration starts following the same process above. The process is repeated until all $y_{k,i}^{(m)}$'s are set to either 0 or 1. The final rate allocation of each link on each channel is calculated according to (10).

STEP 0: Get LP$^{(1)}$ by appending $0 \leq y_{k,i}^{(m)} \leq 1$ to (11) and relaxing all variables to real values.
STEP 1: Solve LP$^{(1)}$.
STEP 2: Pick $Y_{k,i}^{(m)} \Leftarrow \max\{y_{l,j}^{n}, l \in (1, \dots, K), j \in (1, \dots, N), n \in (1, \dots, M)\}$.
STEP 3: Get LP$^{(2)}$ by substituting $Y_{k,i}^{(m)} = 1$, $y_{h,i}^{(m)} = 0$ for $h \neq k$ and $y_{l,j}^{(m)} = 0$ for $\forall j \in I_i$ and $1 \leq l \leq K$ into LP$^{(1)}$.
STEP 4: If LP$^{(2)}$ is feasible
    LP$^{(1)} \Leftarrow$ LP$^{(2)}$
  else
    Get LP$^{(3)}$ by substituting $Y_{k,i}^{(m)} = 0$ into LP$^{(1)}$.
    LP$^{(1)} \Leftarrow$ LP$^{(3)}$
  End-if
STEP 5: If all variables are fixed, then **Terminate**; otherwise go to **STEP 1**.

Table 1: LPSF algorithm.

Theorem 1: The LPSF algorithm can correctly determine the binary values of all $y_{k,i}^{(m)}$'s in no more than NMK iterations.

The proof of Theorem 1 is based on the following lemmas.

Lemma 1: In the first iteration, $\mathrm{LP}^{(1)}$ has an optimal solution.

Proof: It is easy to show that at least $y_{ki}^{(m)} = 0$ for all $k = 1, \ldots, K$, $i = 1, \ldots, N$, and $m = 1, \ldots, M$, is a feasible solution to the original BLP. Thus it is also a feasible solution to $\mathrm{LP}^{(1)}$. Note that all variables are bounded between [0, 1], therefore Lemma 1 holds. ■

Lemma 2: In the first iteration, $\mathrm{LP}^{(3)}$ has an optimal solution.

Proof: According to Lemma 1, $\mathrm{LP}^{(1)}$ in the first iteration must have optimal solution, therefore $Y_{ki}^{(m)} \geq 0$ must holds before the fix. When $Y_{ki}^{(m)}$ is fixed to 0 to get $\mathrm{LP}^{(3)}$, its value is changed from no less than 0 to 0, leading to a non-increase in the required transmission power. So no R.H.S. of C1' through C3' could be violated by this non-increasing action on the L.H.S. of C1' through C3'. Therefore $\mathrm{LP}^{(3)}$ must have at least one feasible solution. Noting that all variables are bounded between [0, 1], Lemma 2 holds. ■

Lemma 3: $\mathrm{LP}^{(1)}$ and $\mathrm{LP}^{(3)}$ have optimal solutions in all iterations.

Proof: The situation in the first iteration is proved by Lemma 1 and Lemma 2. In the second iteration, $\mathrm{LP}^{(1)}$ comes from either a feasible $\mathrm{LP}^{(2)}$ or a feasible $\mathrm{LP}^{(3)}$ of the first iteration. So $\mathrm{LP}^{(1)}$ must be feasible in the second iteration. Given $\mathrm{LP}^{(1)}$ is feasible in the second iteration, the rational used in proving Lemma 2 also applies here to prove the feasibility of $\mathrm{LP}^{(3)}$ in the second iteration. This induction repeats itself in all iterations. Noting that all variables are bounded between [0, 1], Lemma 3 holds. ■

The proof of Theorem 1 is straightforward: Iteratively applying Lemmas 1 to 3, it is guaranteed that in each iteration at least one $y_{ki}^{(m)}$ is fixed to either 0 or 1 and a new feasible $\mathrm{LP}^{(1)}$ is generated for the next iteration. For the last iteration, if fixing $y_{ki}^{(m)}$ to 1 does not lead to a feasible BLP solution, then changing its value to 0 must lead to a feasible BLP solution (due to the same reason as in the proof of Lemma 2). ■

Based on Theorem 1, it is easy to show that the time complexity of the LPSF algorithm is bounded by the complexity of the LP solver times NMK. Because a LP solver has polynomial complexity, the complexity of the LPSF is also polynomial. In addition, the performance gap between the approximate solution and the actual optimum can be explicitly evaluated by comparing against the upper bound of the optimal solution, which is the the solution to $\mathrm{LP}^{(1)}$ in the first iteration. Lemma 1 has guaranteed the existence of this upper bound. We will shortly show by simulation that this gap is very small (below 10%), and in most cases it is zero.

4.3 Distributed Algorithm

In this section, we develop a provably efficient distributed algorithm for the BLP problem (11), which can achieve a provable fraction of the optimal performance. The intuition behind such an algorithm stems from understanding the conflicts between CRs in utilizing spectrum opportunities. There are two main reasons for such conflicts. First, neighboring CRs may observe a similar level of spectrum availability over a given channel, and thus may attempt to transmit simultaneously over the same channel, causing collisions. Second, transmissions by the same CR over different channels may also conflict with each other, in the sense that the maximum transmission power provided by the battery may not be sufficient to support parallel transmissions over all these channels. In a nutshell, conflicts between transmissions occur due to their competition for both frequency and power resources. A good design philosophy is to give priority to a transmission that can contribute higher rate at a lower power. Following this philosophy, the proposed distributed algorithm defines an *economic factor* (EF) for each channel at each CR link. Let the current rate level of link i on channel m be $r_i^{(m)} = u_k$, where $k = 0, \ldots, K-1$. Then, the EF of this channel is defined as

$$\eta_i^{(m)} \stackrel{\text{def}}{=} \frac{\Delta P_i^{(m)}}{B_m \Delta r_i^{(m)}} = \frac{C_i^{(m)}(\gamma_{k+1} - \gamma_k)}{B_m(u_{k+1} - u_k)}. \tag{12}$$

We define $\eta_i^{(m)} \stackrel{\text{def}}{=} +\infty$ for $r_i^{(m)} = u_K$.

The basic idea of our EF-based distributed algorithm is to iteratively ramp up the rate level over each channel of every neighboring link until the power mask and maximum-power constraints are violated. In each iteration, the link-channel pair that has the smallest EF value among its interfering-link set is raised to the next higher rate. This is achieved by sequentially executing the following three procedures in each iteration (note that this algorithm is executed in parallel at various CR transmitters). The first procedure is an *internal candidate selection* process, where a link, say i, selects a channel m^* that has the smallest EF among all channels in a *candidate channel set* $\mathcal{C}$. The set $\mathcal{C}$ is initialized to contain all

```
/* CR link i */
Initialization: r_i^(m) ⇐ 0, for m = 1, ..., M and C ⇐ {1, ..., M}

while (C ≠ ∅ )
   /* Internal candidate selection */
   violation_flag ⇐ 1
   while (violation_flag == 1)
      m* ⇐ arg min { η_i^(m) | m ∈ C }
      calculate ΔP_i^(m*)
      if ((ΔP_i^(m*) + P_i^(m*) ≤ P̂_i^(m*)) or (ΔP_i^(m*) + Σ_{m=1}^{M} P_i^(m) ≤ P_{max,i}))
         violation_flag ⇐ 0
      else
         C ⇐ C−{m*}
      end-if
   end-while

   /* Inter-link selection */
   exchange with neighbors the message (link id i‖channel id m* ‖ η_i^(m*))
   if (η_i^{m*} is the minimum among neighbors)
      increase r_i^(m*) from u_k to u_{k+1}
      if (r_i^(m*) == u_K)
         C ⇐ C−{m*}
      end-if
      send rate-adjustment message
   end-if

   /* Collision elimination routine */
   if (a rate-adjustment message is received from link j)
      calculate h_{S(j)D(i)} based on received signal strength
      if (h_{S(j)D(i)} P̂_j^(m*) > P_{I,CR})
         if (r_i^(m*) ≤ r_j^(m*))
            r_i^(m*) ⇐ 0 and C ⇐ C−{m}
         else
            S(i) sends a rate-adjustment message
         end-if
      end-if
   end-if
end-while
Output: r_i^(m), for m = 1, ..., M
```

Table 2: Pseudo-code for the EF-based distributed algorithm.

M channels. The selected channel m^* is tested for the feasibility of a rate increase: This is done by calculating the increment of transmission power $\Delta P_i^{(m^*)} = C_i^{(m^*)}(\gamma_{k+1} - \gamma_k)$. If this transmission power increment violates the power mask or the battery power constraint, then a rate increase on channel m^* is infeasible for the CR. So m^* will be deleted from $\mathcal{C}$ and the above selection process is repeated. Eventually, either a feasible m^* will be selected or $\mathcal{C}$ becomes empty. When $\mathcal{C}$ becomes empty, the iterative process at the CR transmitter terminates. In case a feasible m^* is found, the algorithm enters the *inter-link selection* phase.

In the inter-link selection phase, neighboring CR transmitters exchange the results of their internal selection to elect the link-channel pair that has the smallest EF among the neighborhood. The internal selection result of a link i is broadcasted in the following format (link id $i \|$channel id $m^* \parallel \eta_i^{(m^*)}$), where $\|$ means concatenation. The link-channel pair that has the smallest EF in its neighborhood raises the corresponding rate by one level, i.e., from u_k to u_{k+1}. At the same time, the sender of this link, say $S(j)$, will broadcast in full power $P_{\max,j}$ the following *rate-adjustment* message to its neighbors: (link id $j \parallel$ channel id $m^* \parallel r_j^{(m^*)} \parallel \hat{P}_j^{(m^*)} \parallel P_{\max,j}$).

Whenever a CR link i receives a rate-adjustment message from link j, it performs a *collision elimination* routine. In particular, the receiver of the ith link, $D(i)$, will calculate the path loss from $S(j)$ (the sender of the message) to $D(i)$ based on the received signal strength of the message. Based on the power mask information in the message, $D(i)$ can then decide whether $S(j)$'s transmission will interfere with the reception at $D(i)$ on channel m. If so, $D(i)$ will compare $r_i^{(m^*)}$ with $r_j^{(m^*)}$. If $r_i^{(m^*)} \le r_j^{(m^*)}$, then $D(i)$ notifies $S(i)$ to set $r_i^{(m^*)}$ to zero and delete m^* from $\mathcal{C}$. If $r_i^{(m^*)} > r_j^{(m^*)}$, then $D(i)$ notifies $S(i)$ to send a rate-adjustment message to trigger link j to eliminate channel m^* from its usage.

A pseudo-code description of the algorithm is given in Table 2. Because at least one $r_i^{(m)}$ will be increased by one level in each iteration in each interfering-link set, the rate adjustment will terminate in at most MK iterations. In addition, Theorem 2 specifies the efficiency of this algorithm.

Theorem 2: The EF-based distributed algorithm can achieve at least $1/(\kappa^* + 1)$ of the optimal performance, where $\kappa^* = \max_{i,m} |I_i^{(m)}|$ is the maximum interference degree of all CR links over all channels, $|\cdot|$ denotes the cardinality of the set.

Proof: The rate adjustment in the EF algorithm is analogous to the well-known single-user optimal Levin-Campello greedy algorithm [13] for bit loading in an OFDM system. In allocating each bit, this greedy algorithm calculates the cost to add one more bit in each subchannel and chooses the subchannel that requires the least cost, where the cost is the incremental power necessary. It has been shown in [9] that for multiuser multi-carrier systems, if we assume no interference exists between users, then the same greedy algorithm also achieves optimal performance. Denote the optimal sum of rate of this idealized non-interfering multiuser system by $R^{(0)}_{tot,\max}$, this sum is calculated as:

$$R^{(0)}_{tot,\max} = \sum_{i=1}^{N} \sum_{m=1}^{M} R_i^{(m)} \tag{13}$$

where $R_i^{(m)}$ are the output of the greedy algorithm when interference between users are ignored. When interference is accounted for, the third "if" statement in the collision-elimination routine of the EF-based algorithm (see Table 2) guarantees that for every interfering link set, only the link that achieves the largest rate is remained (i.e., can access this channel), while all other interfering links are eliminated from using this channel (their rates on this channel are all set to 0). Denote by $Z^{(m)}$ the set of links that can access channel m when the EF algorithm is used. So for $\forall z \in Z^{(m)}$, it must be true that $R_z^{(m)} \geq R_j^{(m)}$ for $\forall j \in I_z^{(m)}$. When interference is accounted for, denote the sum of rate of the EF algorithm by $R^{(1)}_{tot,EF}$. Then $R^{(1)}_{tot,EF} = \sum_{m=1}^{M} \sum_{z \in Z^{(m)}} R_z^{(m)}$. We further have the following relationship:

$$\begin{aligned} R^{(0)}_{tot,\max} &= \sum_{m=1}^{M} \sum_{i=1}^{N} R_i^{(m)} \\ &\leq \sum_{m=1}^{M} \sum_{z \in Z^{(m)}} (|I_z^{(m)}| + 1) R_z^{(m)} \\ &\leq \sum_{m=1}^{M} \sum_{z \in Z^{(m)}} (\kappa^* + 1) R_z^{(m)} \\ &= (\kappa^* + 1) R^{(1)}_{tot,EF} \end{aligned} \tag{14}$$

When interference exists between users, we denote the optimal sum of rate by $R^{(1)}_{tot,\max}$. Obviously,

$$R^{(1)}_{tot,\max} \leq R^{(0)}_{tot,\max} \leq (\kappa^* + 1) R^{(1)}_{tot,EF}. \tag{15}$$

So it follows that $R^{(1)}_{tot,EF} \geq \frac{1}{\kappa^*+1} R^{(1)}_{tot,\max}$. Then Theorem 2 follows. ■

Theorem 2 shows that the EF-based algorithm is optimal when $\kappa^* = 0$, e.g., when any two CR links are separated far away such that they do not interfere with each other. When interference exists, the algorithm's performance lower bound decreases linearly with κ^*. The actual performance gap will be evaluated later on by simulations.

4.4 Additional Constraints

Depending on the CR's hardware capabilities or on some regulatory factors, additional constraints on the CRN may be imposed. These include:

C4: Number of Parallel Transmissions: The maximum number of channels a CR transmitter can use at one time may be bounded by M_t. In the BLP framework, this constraint is presented as

$$\tilde{C}4: \qquad \textstyle\sum_{m=1}^{M} \sum_{k=1}^{K} y^{(m)}_{k,i} \leq M_t, \quad \text{for } i = 1, \ldots, N. \tag{16}$$

C5: Transmission Bandwidth: The total bandwidth a CR can transmit over at one time is bounded by B_t. Formally,

$$\tilde{C}5: \qquad \textstyle\sum_{m=1}^{M} \sum_{k=1}^{K} B_m y^{(m)}_{k,i} \leq B_t, \quad \text{for } i = 1, \ldots, N. \tag{17}$$

C6: Forbidden Channels: A CR link i may be prohibited from using a certain set of channels, say $\mathbf{BF}_i \subseteq \{1, \ldots, M\}$. This constraint can be modeled as

$$\tilde{C}6: \qquad y^{(m)}_{k,i} = 0, \quad \text{for } k = 1, \ldots, K, \text{and } m \in \mathbf{BF}_i. \tag{18}$$

An examination of (16) through (18) shows that the additional constraints are linear in the $y^{(m)}_{k,i}$'s. Thus, they do not fundamentally change the BLP formulation and its solutions discussed in previous sections. The extensions of the LPSF and the EF-based algorithms are trivial, and thus are ignored due to space limitation.

5 Implementation Issues

In this section, we illustrate by an application example the main idea of calculating the multi-level spectrum opportunity. We consider a spectrum-leasing scenario, where a CRN is sharing

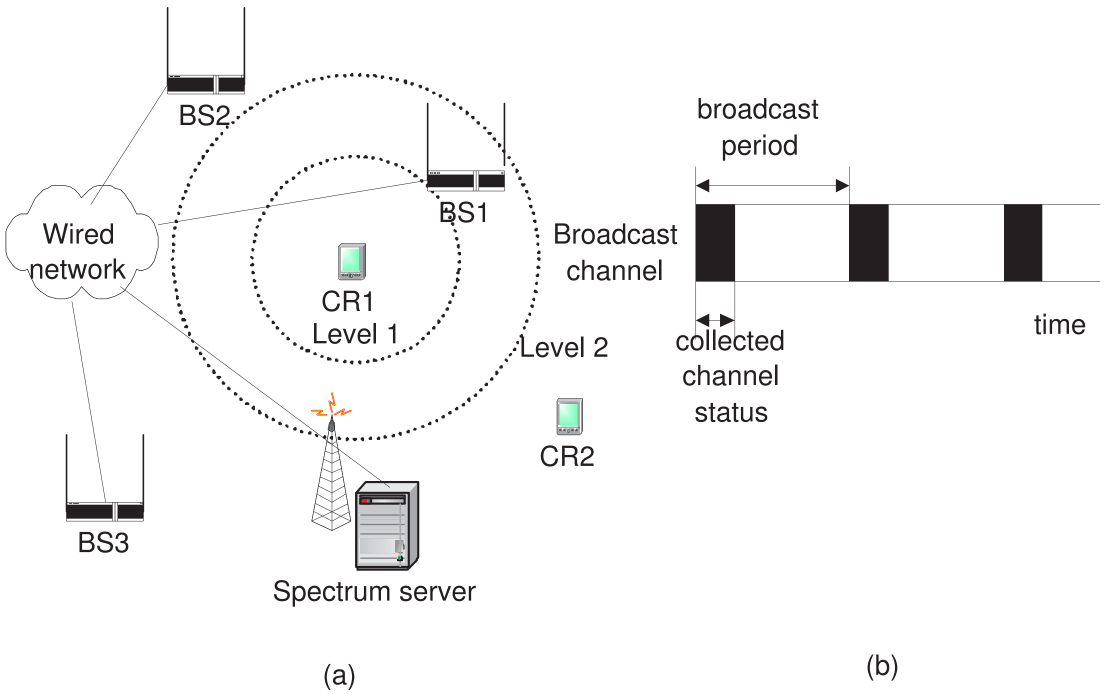

Figure 2: Spectrum leasing: (a) The system structure and (b) Timing of the broadcast of channel-status information from the spectrum server.

spectrum with an infrastructured PRN, as shown in Figure 2. The PRN infrastructure consists of multiple static PR base stations (BSs) that are interconnected via broadband wired network. We assume that the PRN is based on frequency division duplex (FDD) and at any given time, the BS tunes to some of the M uplink channels to receive signal from the PR mobile stations (MSs) (which are not shown in the figure because of its irrelevance with the problem). We only consider the spectrum sharing of the uplink. Note that to be consistent with the model description in Section 3, a BS working on multiple channels can be modeled as multiple virtual BSs working on non-overlapping single channels.

We consider two different spectrum-opportunity discovery mechanisms: (1) Distributed sensing (DS): This is what used in most existing work. Each CR periodically senses channels and discovers binary-type spectrum opportunity. The power mask is either $P_{\max}$ or 0, depending on whether the channel is idle or busy. (2) Subscription-based (SB): Each PR BS periodically reports its status (receiving or idle) on each channel to a spectrum server via the high-speed wired network. The collected real-time channel-status information, along with the location of each BS, is broadcasted by the server to the CRN. By subscribing to the broadcast, each CR can calculate its multi-level spectrum opportunity in the way that we will describe shortly. Besides the throughput gains that will be shown in our simulations, other incentives to use the SB scheme include: First, it provides the spectrum leaser more control over the pricing and regulating of the shared spectrum. Second, because now the sensing functionality can be removed from the CR, its hardware complexity and cost is reduced significantly.

The basic idea of calculating the power mask is to adapt its interference range to the activity of neighboring PR BSs. The interference range is defined as the signal propagation distance d_I, such that $\hat{P}_i^{(m)} h^{(m)}(d_I) \leq P_I$, where $h^{(m)}(d_I)$ is the channel gain for distance d_I on channel m, and the interference tolerance P_I is a small value, below which the interference can be deemed as no harm to the PR. We also assume that each CR has the knowledge of its location, and thus can calculate its distance to neighboring PR BSs. The interference-range adaption is illustrated in Figure 2: If the channel gain is fully decided by the propagation distance, then when BS1 is receiving on channel m, CR1's power mask should be such that its interference range is right smaller than the distance between CR1 and BS1 (denoted as the smallest dotted circle (Level 1) in the figure). When BS1 is not receiving but BS2 is receiving, then the power mask can be increased such that its interference range reaches the larger dotted circle (Level 2), and so on. Although this basic idea seems straightforward, the calculation needs to take into account the following two random factors.

5.1 Randomness of PR Activity

This randomness impacts the choose of right level for the power mask. For example, in Figure 2, even if BS1's status on channel m is reported as not receiving at current reporting time, there is a chance that it subsequently flips to receiving before the next reporting time. This status change cannot be reflected to CRs until the next report. So if a CR is transmitting based on the power mask of Level 2, which is calculated directly according to current status report, then unacceptable interference will be caused to BS1, leading to a violation to the PRN. To account for this random violation, we impose a soft guarantee, $\alpha^{(m)}$ for channel m, such that the ratio of the time the CR violates PRN on channel m is smaller than $\alpha^{(m)}$. This constraint requires us to take into account the accumulated possibility of status-flipping (from not-receiving to receiving) of all idle BSs that are closer to the target CR than its closest active BS neighbor. As a result, it might not always be appropriate to use a power mask that corresponds to the closest active BS neighbor. For example, in Figure 2, even if BS2 is the closet active neighbor of CR1 in the current report, the CR should not use the power mask of Level 2, if the possibility of BS1 flipping to receiving is greater than $\alpha^{(m)}$. Mathematically, this problem is formulated as solved as follows.

We use the calculation on channel m as an illustration. For a target CR, label its PR BS neighbors from close to far (BS 1 is the closest to the CR). Denote its power mask set on channel m by $\mathbf{p}_{mask}^{(m)} = (p_{mask}^{(m)}(1), p_{mask}^{(m)}(2), \ldots, p_{mask}^{(m)}(N_m+1))$, where $p_{mask}^{(m)}(j) = P_I/h_j^{(m)}$ for $j = 1, \ldots, N_m$, $h_j^{(m)}$ is the path loss from the target CR to its j PR BS neighbor and $h_1^{(m)} \geq \ldots \geq h_{N_m}^{(m)}$, the N_mth BS neighbor is the one beyond which the CR-to-PR interference is always smaller than P_I even if the CR is transmitting on its full power $P_{\max}$. We also define $p_{mask}^{(m)}(N_m+1) \stackrel{\text{def}}{=} P_{\max}$. Define the channel-usage profile at the nth reporting time as a N_m-dimensional vector $\mathbf{S}^{(m)}(n) = (s_1^{(m)}(n), \ldots, s_{N_m}^{(m)}(n))$, where for $i = 1, \ldots, N_m$:

$$s_i^{(m)}(n) = \begin{cases} 1, & \text{if BS } i \text{ is receiving at the } n\text{th report} \\ 0, & \text{if BS } i \text{ is not receiving at the } n\text{th report} \end{cases} \tag{19}$$

Denote the status of BS i by random process $x_i^{(m)}(t)$: $x_i^{(m)}(t) = 1/0$ denotes the receiver is receiving (ON)/not-receiving (OFF) at time t. Let τ_n and τ_{n+1} denote the nth and the $(n+1)$th status reporting time, respectively. So $s_i^{(m)}(n)$ denote the value of $x_i^{(m)}(t)$ at time τ_n. Define a new random variable $\xi_i^{(m)}$ as follows:

$$\xi_i^{(m)} = \begin{cases} 1, & \text{if } x_i^{(m)}(t) = 1 \text{ for some } t \in [\tau_n, \tau_{n+1}] \\ 0, & \text{if } x_i^{(m)}(t) = 0 \ \forall t \in [\tau_n, \tau_{n+1}]. \end{cases} \tag{20}$$

The dynamics of $x_i^{(m)}(t)$ between τ_n and τ_{n+1} can take one of four possible cases, as illustrated in Figure 3. Using the current sensing time τ_n as the reference point, we denote the forward recurrence time of the OFF state by $\tilde{T}_{OFF}$ and the forward recurrence time of the ON state by $\tilde{T}_{ON}$. Following standard results in renewal theory [4], the probability of each case can be calculated as follows:

$$\Pr\left\{\xi_i^{(m)} = 0 | s_i^{(m)}(n) = 0\right\} = \Pr\left\{\tilde{T}_{OFF} > T\right\} = 1 - \int_0^T f_{\tilde{T}_{OFF}}(t)dt \tag{21}$$

$$\Pr\left\{\xi_i^{(m)} = 1 | s_i^{(m)}(n) = 0\right\} = \Pr\left\{\tilde{T}_{OFF} \leq T\right\} = \int_0^T f_{\tilde{T}_{OFF}}(t)dt \tag{22}$$

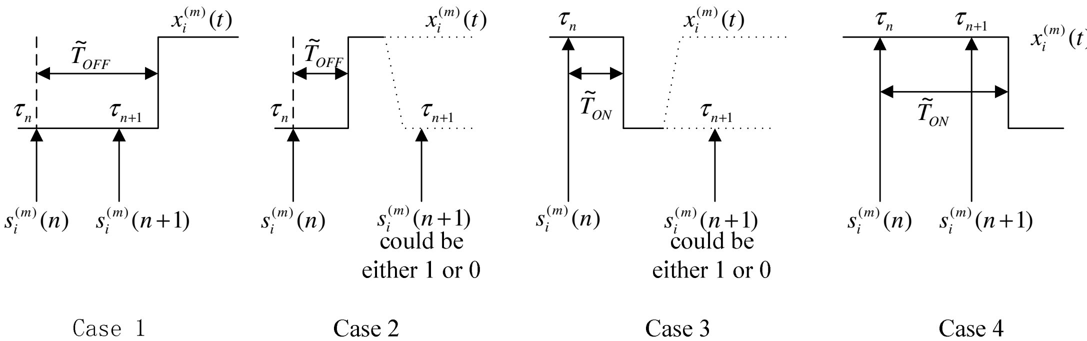

Figure 3: Randomness of PR activity.

$$\Pr\left\{\xi_i^{(m)} = 0 | s_i^{(m)}(n) = 1\right\} = 0 \tag{23}$$

$$\Pr\left\{\xi_i^{(m)} = 1 | s_i^{(m)}(n) = 1\right\} = 1 - \Pr\left\{\xi_i^{(m)} = 0 | s_i^{(m)}(n) = 1\right\} = 1 \tag{24}$$

where $T \stackrel{\text{def}}{=} \tau_{n+1} - \tau_n$ is the sensing period and $f_{\tilde{T}_{OFF}}(t)$ is the pdf of $\tilde{T}_{OFF}$, which can be derived from the pdf of the OFF period $f_0^{(m)}$:

$$f_{\tilde{T}_{Off}}(t) = \frac{1 - \int_0^t f_0^{(m)}(\tau) d\tau}{\int_0^\infty \tau f_0^{(m)}(\tau) d\tau}. \tag{25}$$

Note that (23) can be justified by observing the definition of the r.v. $\xi_i^{(m)}$ in (20). At time τ_n, given a sensing output $\mathbf{S}^{(m)}(n)$, the violation probability of the CR transmitter on channel m is conditioned on the power mask to be used. Because the neighboring PR receivers $v_i^{(m)}$'s are labeled in the descending order of their channel gains, at a given power-mask level l $(1 \leq l \leq N_m + 1)$, a violation will happen if and only if there exists at least one PR neighbor i, $i < l$, for which $\xi_i^{(m)} = 1$. Mathematically, the violation rate for a given level of power mask can be calculated as follows:

$$\begin{aligned}
& \Pr\{\text{violation of PRN } m | \mathbf{S}^{(m)}, p_{mask}^{(m)}(l)\} \\
= \;& \Pr\{\xi_1^{(m)} = 1 | \mathbf{S}^{(m)}\} + \Pr\{\xi_1^{(m)} = 0, \xi_2^{(m)} = 1 | \mathbf{S}^{(m)}\} \\
& + \ldots + \Pr\{\xi_1^{(m)} = 0, \ldots, \xi_{l-2}^{(m)} = 0, \xi_{l-1}^{(m)} = 1 | \mathbf{S}^{(m)}\} \\
= \;& \Pr\{\xi_1^{(m)} = 1 | s_1^{(m)}\} + \Pr\{\xi_1^{(m)} = 0 | s_1^{(m)}\} \Pr\{\xi_2^{(m)} = 1 | s_2^{(m)}\} \\
& + \ldots + \Pr\{\xi_1^{(m)} = 0 | s_1^{(m)}\} \Pr\{\xi_2^{(m)} = 0 | s_2^{(m)}\} \\
& \times \ldots \times \Pr\{\xi_{l-2}^{(m)} = 0 | s_{l-2}^{(m)}\} \Pr\{\xi_{l-1}^{(m)} = 1 | s_{l-1}^{(m)}\}.
\end{aligned} \tag{26}$$

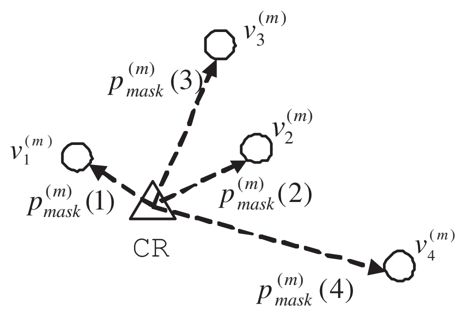

Figure 4: An example of run-time spectrum opportunity detection.

The multiplicative form in the last step of (26) is due to the independence between different PR links. We can rewrite (26) in a compact form as

$$V(l, \mathbf{S}^{(m)}) \stackrel{\text{def}}{=} \sum_{i=1}^{l-1} \Pr\{\xi_i^{(m)} = 1 | s_i^{(m)}\} \prod_{j=1}^{i-1} \Pr\{\xi_j^{(m)} = 0 | s_j^{(m)}\} \tag{27}$$

for $l = 1, \ldots, N_m + 1$. In addition, we also define $V(N_m + 2, \mathbf{S}^{(m)}) = 1$. The conditional probabilities $\Pr\{\xi_i^{(m)} | s_i^{(m)}\}$ in (27) can be computed according to (21) through (24). The level of spectrum opportunity l^* over channel m should be selected such that $V(l^*, \mathbf{S}^{(m)}) \leq \alpha^{(m)}$ and $V(l^* + 1, \mathbf{S}^{(m)}) > \alpha^{(m)}$. It is easy to verify that $V(l, \mathbf{S}^{(m)})$ defined in (27) is a mono-increasing function of l. Thus this selection is valid in the sense that some l^* can always be found. Then the power mask of the target CR, say CR i, is simply $\hat{P}_i^{(m)} = p_{mask}^{(m)}(l^*)$.

As an example of the above calculation, consider the scenario in Figure 4, where the CR has four PR BS neighbors channel m. Assume the pdf function f_0 is exponential with a mean of 10 s, and the broadcast period is 100 ms. The translation from a the channel-usage profile ($s_i^{(m)}$ corresponds to PR BS $v_i^{(m)}$) to the level of maximum allowable power mask, l^*, is calculated in Table 3 for the cases of $\alpha = 1\%$ and $\alpha = 2\%$, respectively.

5.2 Randomness of the Channel Gain

This randomness impacts the value of each power mask level. Given $\hat{P}_i^{(m)}$, the random fluctuation of the channel makes the received signal strength after distance d_I a random variable: $\hat{p}_i^{(m)} = \hat{P}_i^{(m)} \bar{h}(d_I) \chi^{(m)}$, where $\chi^{(m)}$ is a unit-mean r.v. denoting the random fluctuation of the channel, $\bar{h}(d_I) = A_0 d_I^{-\mu}$ is the distance-related component of path loss, A_0 is the close-in constant, and μ is the path loss exponent. To counter this random effect, we impose a second

$(s_1^{(m)} s_2^{(m)} s_3^{(m)} s_4^{(m)})$	l^* $(\alpha = 1\%)$	l^* $(\alpha = 2\%)$
(0000)	1	3
(0001)	1	3
(0010)	1	3
(0011)	1	3
(0100)	1	2
(0101)	1	2
(0110)	1	2
(0111)	1	2
(1000)	1	1
(1001)	1	1
(1010)	1	1
(1011)	1	1
(1100)	1	1
(1101)	1	1
(1110)	1	1
(1111)	1	1

Table 3: Mapping between channel-usage profile and run-time opportunity.

soft guarantee, $\beta^{(m)}$ for channel m, which requires $\Pr\{\hat{P}^{(m)}\bar{h}(d_I)\chi^{(m)} \geq P_I\} < \beta^{(m)}$. Since d_I is fixed (this corresponds to the interference range of the level selected in last section), $\hat{P}_i^{(m)}$ is calculated as $\hat{P}_i^{(m)} = \frac{P_I}{\bar{h}(d_I)Q^{(m)}(\beta^{(m)})}$, where $Q^{(m)}(\beta^{(m)})$ is the $(1-\beta^{(m)})$-quantile of the fluctuation $\chi^{(m)}$, i.e., $\Pr\{\chi^{(m)} \leq Q^{(m)}(\beta^{(m)})\} = 1 - \beta^{(m)}$.

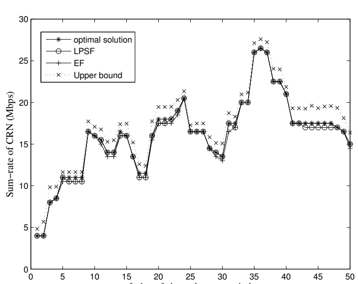

Figure 5: Trace of the CRN's Sum-rate.

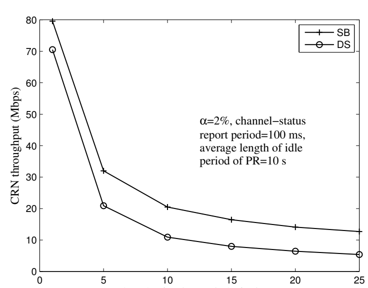

Figure 6: CRN throughput vs. PR activity.

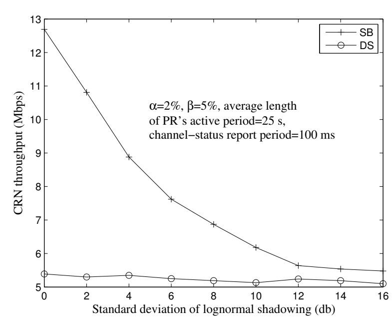

Figure 7: CRN throughput vs. channel shadowing.

Obviously, the frequency by which each BS reports to the spectrum server has an impact on the calculated power mask. The lower the frequency, the larger the uncertainty for the BS' status between two consecutive reports, and therefore the more conservative the power mask will be in order to guarantee the given PRN violation constraint. On the other hand, the bandwidth of the channel-status information broadcast channel also influences the throughput of the CRN: Because CRs update their power masks according to the periodic broadcast, the higher the broadcast bandwidth, the quicker each CR can acquire the channel-status information, thus more time left between two consecutive updates for a CR to deliver data. The interesting question is how much gain the multi-level scheme can attain when the overhead of the broadcast has been accounted for. We will answer this question based on simulations shortly.

6 Performance Evaluation

6.1 Accuracy of the Approximate Algorithms

We consider a 1000×1000 meter^2 region, where 5 PRNs (5 channels) coexist with 5 CR links. The numbers of PRs over each channel are 25, 10, 15, 20, and 25, respectively. Each channel has 1 MHz of bandwidth. We assume the following rate-SINR relationship: $R_i^{(m)} = B_m \log_2(1 + SINR/8)$, and $r_i^{(m)} \in \{0, 1/2, 1, 3/2, 2\}$ bits/second/Hz for all i and m. The locations of the PR and CR transmitters and receivers are randomly assigned within the simulation region. A simple path loss model with exponent of 4 is assumed for the channel gain between any two points (i.e., $h_{ij} = d_{ij}^{-4}$). We assume the PRs on all channels follow the same 2-state Markov activity model, i.e., durations of ON/OFF states are exponentially distributed, with the average ON and OFF periods set to 1 s and 10 s, respectively. The transmission power of a PR is 500 mW. The $P_{\max}$ for a CR is 1 W. We assume the interference tolerance $P_I = 2P_{I,CR} = 0.12346$ μW. The power masks of all CRs are calculated periodically according to the SB scheme. The PR's status report period is 100 ms and the CR-to-PR violation bound is $\alpha^{(m)} = 2\%$ for all m. A CR is capable of using all 5 channels at one time. We compare the sum-rate of all CR links achieved in each report period under 3 different algorithms: an exhaustive-search algorithm that finds the optimal solution, our polynomial-time LPSF algorithm, and the EF algorithm.

The CRN sum-rate is plotted in Figure 5 for 50 consecutive status report periods. We randomly choose to present this trace among the many we have simulated. The upper bound generated in the first iteration of the LPSF algorithm is also shown. It is clear that the LPSF and the EF algorithms give near-optimal solutions. In all cases, these solutions are within 5%

from the optimal solution. In most of the cases their solution is the actual optimal solution. In addition, the upper bound provided by the LPSF algorithm is reasonably tight. In all simulations, the gap between this bound and the optimal solution does not exceed 10%. So this bound provides a useful reference to evaluate the accuracy of the approximate solutions in large networks when the optimal solution is computationally difficult to obtain.

6.2 Comparison between Binary and Multi-level Opportunity

Since getting the optimal solution is not our target in this section, we simulate a larger-scale system and apply EF algorithm for channel access. We consider 10 channels and 10 CR links over the same square area. The numbers of PRs on each channel are 25, 10, 15, 20, 25, 10, 5, 15, 20, and 25, respectively. In addition, the set of rates supported by a CR is now given by $\{0, 1/2, 1, 3/2, 2, 5/2, 3, 7/2, 4\}$ b/s/Hz. So the number of binary variables in the BLP is increased to 800. Unless indicated, the other parameters stay the same as before. The results presented below are based on the average of 20 randomly generated topologies, with a simulation time of 1000 sensing/status-report periods for each topology.

We assume the channel-sensing period of DS scheme is 100 ms. We denote the status-report period of SB scheme by T. The performance matric of interest is the CRN throughput, defined as the average number of data bits that can be transmitted by all CR links in one period divided by the duration of the period. Because under the SB scheme, a fraction of the period, denoted by T_B, is used to receive broadcast information at each CR, the actual data transmission time in each period is $T - T_B$. The overhead is given by $T_B = \frac{V_B}{B_B}$, where V_B is the number of bits of the collected channel-status information in one report period, and B_B is the bandwidth of the broadcast channel. For our simulation, V_B is loosely upper bounded as follows: We assume that the channel-status information for one PR has the format (PR id $\|$ channel id $\|$ channel status). The total number of PRs is less than 200, so an id of 8 bits is enough to identify each of them. The total number of channels is 10, so 4 bits are enough to identify the channel a PR is working on, and 1 bit is used to identify the status of the PR (ON/OFF). So $V_B < 200 \times (8 + 4 + 1) = 2.6K$ bits. We use this value in our following calculation of the overhead. To give a conservative estimation of the gain attained by SB scheme, we assume that the channel sensing in DS scheme takes 0 time. Thus the throughput of the DS scheme plotted below represents the upper bound of any channel access schemes that are based on binary spectrum opportunity. We ignore the EF algorithm's computation time in both schemes.

In Figure 6, we study the CRN throughput as function of the PRs' activities. Here we fix $B_B = 260$ Kb/s, corresponding to $T_B = 10$ ms. It can be observed that at low PR activity, the throughput of SB exceeds DS slightly (a 15% gain); but at high PR activity, SB exceeds DS significantly (a 150% gain). So it is clear that although the broadcast channel consumes about 2.6% of the total system bandwidth, it leads to at least 15% throughput gain in worst case and 150% gain in best case scenarios. The difference of gains is because when PR activity is low, all neighboring PRs are often in the OFF state. The outcome of SB becomes similar to DS in the sense that most of the time a CR can use the highest power level $P_{\max}$ for transmission. With increased PR activity, the middle- and low-level power masks happen more and more frequently under the SB scheme, while DS observes more and more "0" (no transmission) opportunities, thus the gap between the two schemes keeps growing.

We study the impact of channel fluctuations in Figure 7, where a channel is subject to log-normal shadowing. The channel gain is now simulated by $g_{ij} = d_{ij}^{-4} 10^{\frac{\chi}{10}}$, where χ is a zero-mean Gaussian random variable denoting the channel fluctuation measured in decibel (db). The standard deviation of χ represents the severity of the shadowing. For each channel, we require the soft guarantee $\beta = 5\%$. We first note that the average throughput of DS barely changes with the fluctuation because it has a fixed power-mask set $(0, P_{\max})$. It is also observed that with the increase of channel fluctuation, the throughput under SB will decrease, and eventually it approaches to that of TOS. But when the standard deviation is 6 db, which is the value for a typical shadowing environment, SB still achieves about 50% throughput gain over DS.

In Figure 8, we fix $B_B = 260$ Kb/s (or $T_B = 10$ ms) and change the status-broadcast period as the variable. It can be observed that in general, a shorter broadcast period leads to a higher throughput because of the increased certainty of the PR's activity between two consecutive reporting moments. However, when the broadcast period is very small, e.g., $T = 40$ ms, the throughput of SB is low. This is because the broadcast of status information occupies a significant portion of each broadcast period, thus less time is left for

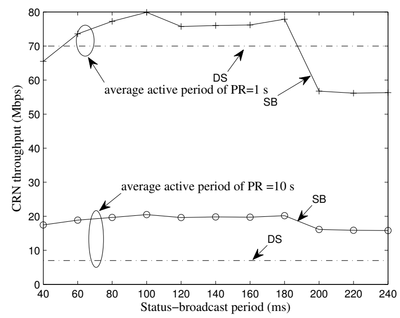

Figure 8: CRN throughput vs. period of the status broadcast.

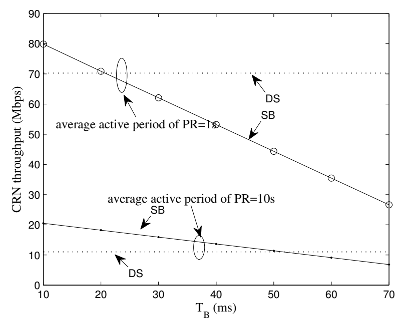

Figure 9: CRN throughput vs. bandwidth of the broadcast channel.

data transmission.

In Figure 9, we fix the status-broadcast period $T = 100$ ms, and plot the throughput of SB under various T_B (corresponding to various broadcast channel bandwidth). It can be observed that the throughput of SB degrades linearly with the increase of T_B (or equivalently, the decrease of the broadcast bandwidth), because less and less fraction of time in each period is left for transmitting data. For low PR activity, the throughput of SB crosses that of DS after T_B is greater than 20 ms or B_B is smaller than 130 Kb/s, which is about 1.3% of the total system bandwidth. For high PR activity, the crossing point is $T_B = 50$ ms. This corresponds to $B_B \approx 50$ Kb/s (0.5% of the total bandwidth). The extremely small bandwidth at the crossing in both situations indicate that the overhead of SB is basically ignorable compared with the significant throughput gains it leads to.

7 Conclusions

In this paper, we developed both centralized and distributed algorithms to solve the joint power/rate control and channel assignment problem for the coordinated channel access in CRNs. The problem is formulated under a multi-level spectrum opportunity framework that reflects the microscopic spatial opportunity available for CRs. We also applied our algorithms to study the throughput gains achieved by this multi-level framework over the conventional binary ones while taking its overhead into account. We showed that significant gains can be achieved under the assistance of a narrow-band channel, which periodically broadcasts channel-status information to facilitate CRs calculating their multi-level spectrum opportunity. Currently our work only applies to single-hop ad hoc CRNs. Our future efforts will include the routing into the problem for a multi-hop environment.

References

[1] L. Cao and H. Zheng. Distributed spectrum allocation via local bargaining. In *Proceedings of IEEE Communications Society Conference on Sensor, Mesh and Ad Hoc Communications and Networks SECON*, 2005.

[2] L. Cao and H. Zheng. On the efficiency and complexity of distributed spectrum allocation. In *Proceedings of International Conference on Cognitive Radio Oriented Wireless Networks and Communications*, 2007.

[3] N. B. Chang and M. Liu. Optimal channel probing and transmission scheduling for opportunistic spectrum access. In *Proceedings of the ACM MobiCom Conference*, 2007.

[4] D. R. Cox. *Renewal Theory*. Butler & Tanner Ltd., 1967.

[5] Y. T. Hou, Y. Shi, and H. D. Sherali. Optimal spectrum sharing for multi-hop software defined radio networks. In *Proceedings of the IEEE INFOCOM Conference*, pages 1–9, 2007.

[6] S. Huang, X. Liu, and Z. Ding. Opportunistic spectrum access in cognitive radio networks. In *Proceedings of the IEEE INFOCOM Conference*, pages 1427–1435, Apr. 2008.

[7] J. Jia, Q. Zhang, and X. Shen. HC-MAC: a hardware-constrained cognitive mac for efficient spectrum management. *IEEE Journal on Selected Areas in Communications*, 26(1):106–117, Jan. 2008.

[8] H. Kim and K. G. Shin. Efficient discovery of spectrum opportunities with mac-layer sensing in cognitive radio networks. *IEEE Transactions on Mobile Computing*, 7(5):533–545, May 2008.

[9] J. Lee, R. V. Sonalkar, and J. M. Cioffi. Multiuser bit loading for multicarrier systems. *IEEE Transactions on Communications*, 54(7):1170–1174, July 2006.

[10] Y. Shi and Y. T. Hou. Optimal power control for multi-hop software defined radio networks. In *Proceedings of the IEEE INFOCOM Conference*, pages 1694–1702, 2007.

[11] Y. Shi and Y. T. Hou. A distributed optimization algorithm for multi-hop cognitive radio networks. In *Proceedings of the IEEE INFOCOM Conference*, pages 1966–1974, Apr. 2008.

[12] Y. Shi, Y. T. Hou, H. D. Sherali, and S. F. Midkiff. Optimal routing for uwb-based sensor networks. *IEEE Journal on Selected Areas in Communications*, 24(4):857–863, Apr. 2006.

[13] T. Starr, M. Sorbara, J. M. Cioffi, and P. J. Silverman. *DSL Advances*. Prentice-Hall, 2003.

[14] W. Wang and X. Liu. List-coloring based channel allocation for open-spectrum wireless networks. In *Proceedings of the IEEE Vehicular Tech. Conference*, pages 690–694, 2005 Fall.

[15] Y. Xing, R. Chandramouli, S. Mangold, and S. N. Shankar. Dynamic spectrum access in open spectrum wireless networks. *IEEE Journal on Selected Areas in Communications*, 24(3):626–637, Mar. 2006.

[16] Y. Xing, C. N. Mathur, M. A. Haleem, R. Chandramouli, and K. P. Subbalakshmi. Dynamic spectrum access with qos and interference temperature constraints. *IEEE Transactions on Mobile Computing*, 6(4):423–433, Apr. 2007.

[17] Y. Yuan, P. Bahl, R. Chandra, T. Moscibroda, and Y. Wu. Allocating dynamic time-spectrum blocks in cognitive radio networks. In *Proceedings of the ACM MobiHoc Conference*, pages 130–139, 2007.

[18] J. Zhao, H. Zheng, and G. Yang. Distributed coordination in dynamic spectrum allocation networks. In *Proceedings of the IEEE Symposium on New Frontiers in Dynamic Spectrum Access Networks (DySPAN)*, 2005.

[19] Q. Zhao, S. Geirhofer, L. Tong, and B. M. Sadler. Optimal dynamic spectrum access via periodic channel sensing. In *Proceedings of the IEEE WCNC Conference*, 2007.

[20] Q. Zhao, L. Tong, A. Swami, and Y. Chen. Decentralized cognitive mac for opportunistic spectrum access in ad hoc networks: A POMDP framework. *IEEE Journal on Selected Areas in Communications*, 25(3):589–600, Apr. 2007.

[21] H. Zheng and L. Cao. Device-centric spectrum management. In *Proceedings of the IEEE Symposium on New Frontiers in Dynamic Spectrum Access Networks (DySPAN)*, 2005.

[22] H. Zheng and C. Peng. Collaboration and fairness in opportunistic spectrum access. In *Proceedings of the IEEE ICC Conference*, 2005.